Operating Field Optimization of Giant Magneto Impedance (GMI) Devices in Micro Scale for Magnetic Bead Detection

Dohun Kim[1,2], Hyungkyung Kim[1], Sunhee Park[1], Wooyoung Lee[2], and Won Young Jeung[1]

[1]Division of Material Research, Korea Institute of Science and Technology, Hawolgok Dong, Seongbuk Gu, Seoul 136-791, Korea

[2]Department of Materials Science and Engineering, Yonsei University, Chinchon Dong, Seodaemun Gu, Seoul 120-749, Korea

Giant magneto impedance (GMI) effect devices for magnetic bead detections were examined. Since commercialized magnetic beads in biological applications are superparamagnetic in nature, not only for improvement of maximum sensitivity but also precise optimizations of operating fields are crucial for sensor applications. We have found that operating fields and maximum sensitivity can be enhanced by the tailoring aspect ratio in microscopic GMI sensors. With an aspect ratio of 3.3–3.8, the GMI sensors were found to exhibit an overall GMI ratio of more than 110% and a maximum sensitivity of 1.61 mV/Oe (15.4%/Oe) at the operating field of 43.1 Oe. Our results demonstrate that microscopic GMI sensors are highly sensitive to magnetic bead detections.

***Index Terms*—Magnetic bead detection, magneto impedance, root-mean-square (rms)-to-dc conversion, skin effect, uniaxial anisotropy.**

I. Introduction

THE SENSITIVE measurement of localized magnetic field has been a growing issue in applied magnetism because of its possibility for biological applications, such as protein detection and onchip cytometer. To this end, using conventional magnetic sensors, such as the Hall effect, giant magneto resistance (GMR), and magnetic tunnel junction (MTJ) sensors, various methods to dynamically detect micron-sized magnetic beads have been proposed. [1]–[3] According to [1], for ferrite-based magnetic bead detection, the field resolution of < 1 Oe is required and they demonstrated dynamic detection of a single magnetic bead using the MTJ sensor which has a sensitivity of 0.4%/Oe at 15 Oe of the external magnetic field.

Meanwhile, a giant magneto impedance (GMI) effect, which implies a sensitive change of impedance of soft magnetic materials with an external magnetic field, has been known to have ultra-high sensitivity compared to GMR or MTJ sensors [5]–[7], the property with which a successful biological application would be feasible. Conventional GMI devices, however, are fabricated mainly by the melt-spinning method and due to difficulty of miniaturization with this method, they typically have millimeter dimensions. Moreover, as the operating frequency exceeds well over MegaHertz and output power reaches down to nanowatts in microscale, the successful measurement requires wide bandwidth and resolution; otherwise, one cannot exploit the full capacity of microscaled GMI sensors.

In this paper, we have investigated GMI effect sensors in microscale which are fabricated using $Co_{30}Fe_{34}Ni_{36}$ electroplated microwires. Since common magnetic beads in biological applications are superparamagnetic in nature, sensors that show maximum sensitivity at a relatively large applied field are advantageous for bead detection. By optimizing the aspect ratio, we have successfully fabricated a microscopic GMI sensor with a total MI ratio of more than 110% and a maximum sensitivity of 1.609 mV/Oe (15.4%/Oe) at the magnetic field of 43.1 Oe, showing the possibility of application to highly sensitive biosensors.

TABLE I
VARIATION OF LATERAL DIMENSIONS

Sample	Width (w)	Length (l)	Aspect Ratio
1	27.8	260.8	9.3
2	38.5	268.7	6.9
3	66.3	258.5	3.8
4	74.6	248.8	3.3

All units are in micro meters. Thickness of all devices was fixed to be 1.5 um .

II. Experiment

In previous works, we examined the various effects of electroplating conditions on the soft magnetic property of CoFeNi alloys [13]–[15]. With an optimized condition, $Co_{30}Fe_{34}Ni_{36}$ soft magnetic alloys that have transverse uniaxial magnetic anisotropy were electroplated on silicon substrates. In order to investigate GMI characteristics depending on aspect ratios of the devices, microwire patterns having dimensions of width: 25–75 μm, length: 230–270 μm, and thickness: 1.5 μm were formed by using the conventional photolithography method and were wet etched subsequently. The length of the active area was fixed to 20 μm. Four probe electrodes for electrical measurements were formed by RF magnetron sputtering. Various device dimensions used in this paper are summarized in Table I. Soft magnetic properties were characterized by measuring the hysteresis loop with a Lakeshore 7400 vibrating sample magnetometer (VSM), from which the coercivity of the $Co_{30}Fe_{34}Ni_{36}$ was found to be less than 0.2 Oe and the transverse magnetic anisotropy was confirmed. From Kelvin four-probe IV measurements, the typical dc resistances of the devices were found to be in range from 0.07 Ω to 0.15 Ω, depending on the area of the active regions.

Digital Object Identifier 10.1109/TMAG.2008.2002611

Color version of one or more of the figures in this paper are available online at http://ieeexplore.ieee.org.

Conventionally, the impedance profile at high frequencies is determined by measuring the reflection coefficient with network analyzers. Although total impedances of present devices are expected to be larger than dc resistances at high frequencies, their values are too low to be measured accurately by this method since network analyzers are typically optimized for 50- or 75-Ω electrical networks [4]. More important, since it is the output voltage, which is ultimately used for the sensor application, we used the sensor's root mean square (rms) voltage signal for the magnetic impedance ratio evaluation according to the following formula:

$$\mathrm{GMI}(\%) = \frac{V_{\mathrm{rms}}(H) - V_{\mathrm{rms}}(0)}{V_{\mathrm{rms}}(0)} \quad (1)$$

where $V_{\mathrm{rms}}(H)$ and $V_{\mathrm{rms}}(0)$ represent the sensor output rms voltage with an applied magnetic field and zero magnetic field, respectively. We used the Agilent 33220A function generator as an RF sine-wave signal source, of which source the RF power is set to be approximately 7 dBm (5 mW) for all measurements.

Fig. 1 shows the schematic block diagram of detecting sensor output. Magneto impedance sensors basically utilize ac signals which must be converted to the dc value for sensor applications. In [10], depending on the measurement scheme and operating temperature, a direct Schottky diode or synchronized rectification using an analog switch was adapted in the sensor circuitry. Since it is needed to improve the minimum detectable voltage as the device dimension is reduced down to microscale, we adapted the rms-to-dc conversion technique for detecting the sensor output using Analog Devices' AD8361 RF detector integrated-circuit (IC) chip. Inside the AD8361's transconductance cell, the RF signal from the GMI sensor induces thermal energy which is transformed into dc voltage that is directly proportional to the rms value of the signal. Then, the resulting dc voltage can be easily amplified with an instrumentation amplifier having a high common-mode rejection ratio (CMRR) in order to increase the SNR and be measured using A conventional digital multimeter (DMM) with high accuracy. The overall gain of the measurement system was set to be approximately 20 dB (ten times). Due to its inherent large bandwidth and high resolution, it is expected that the rms-to-dc conversion scheme is adequate for microscale GMI measurement.

III. Result and Discussion

Since the detection of the super paramagnetic beads utilizes stray dipole fields from the beads, measurement is commonly performed with an applied magnetic field, called the operating field, where the sensor shows maximum sensitivity. Since the stray field increases along with the applied field, it may be advantageous to have a large operating field. On the other hand, when this field is too large, undesirable effects, such as particle aggregation occur. Therefore, for the magnetic bead sensor application, not only is there animprovement of maximum sensitivity but also precise optimization of the operating field is important.

It is well known from previous works [4]–[8] that the GMI effect stems from the following effects depending on the

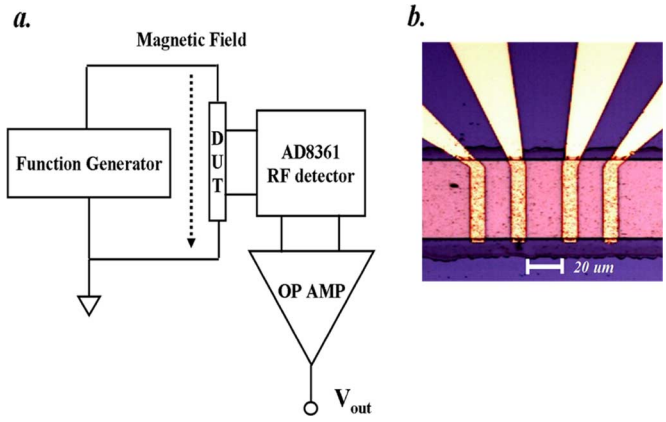

Fig. 1. (a) Schematic diagram of the RF power measurement using the AD8361 RF detector IC. (b) Microscope image of a typical GMI sensor used in this paper. The length between the voltage-sensing electrode was fixed to 20 μm.

frequencies of exciting ac signals. First, below the megahertz region, a variation of inductive reactance dominates the total impedance changes under the applied magnetic field. This effect is called the magneto inductive effect [4]. In this regime, device impedance shows the maximum value at zero magnetic fields and decreases monotonically as the applied magnetic field increases. Despite the reported high sensitivity [4], [5] at this low frequency, however, the operating frequency cannot be set to this regime because magnetic beads hardly emanate the stray field due to the near zero operating field.

In contrast, in microwave frequencies above 1 GHz, ferromagnetic resonance (FMR) contributes to the impedance profile and impedance maximum occurs at a relatively large magnetic field. However, too large of an operating field and broadening of the impedance peak around the resonance field inhibits setting the operating frequency at this regime. Therefore, we set the operating frequency in the radio-frequency (RF) region, that is, from 1 MHz to 300 MHz. In this regime, the severe eddy current inhibits the domain wall motion so that magnetization rotation mainly determines the magnetization process. Also, due to the skin effect, an applied electromagnetic field is concentrated at the surface of the material [6]–[8]. This increased surface contribution largely modifies an impedance profile so that the GMI ratio increases well above a few tens of percent and typically has a reasonable operating field.

Fig. 2 shows the MI profiles of micron-scaled sensors fabricated in this paper. In the RF frequency regime, the typical impedance profile shows double peak behavior as an external applied magnetic field is swept from negative maximum to positive maximum value [6], [8]. In Fig. 2, for the purpose of clarity, impedance profiles in the positive magnetic-field region are presented. As total impedances of active area of the devices are typically much less than 1 Ω, almost the entire incident signal is reflected back to the signal source and the rms voltage across the device active area at zero magnetic field was found to be approximately 1 mV (−47 dBm). Beginning with this value, the maximum rms voltage reached approximately 2.2 mV (−40.1 dBm). According to these rms voltage measurements, the typical MI ratio of our devices with respect to the external magnetic

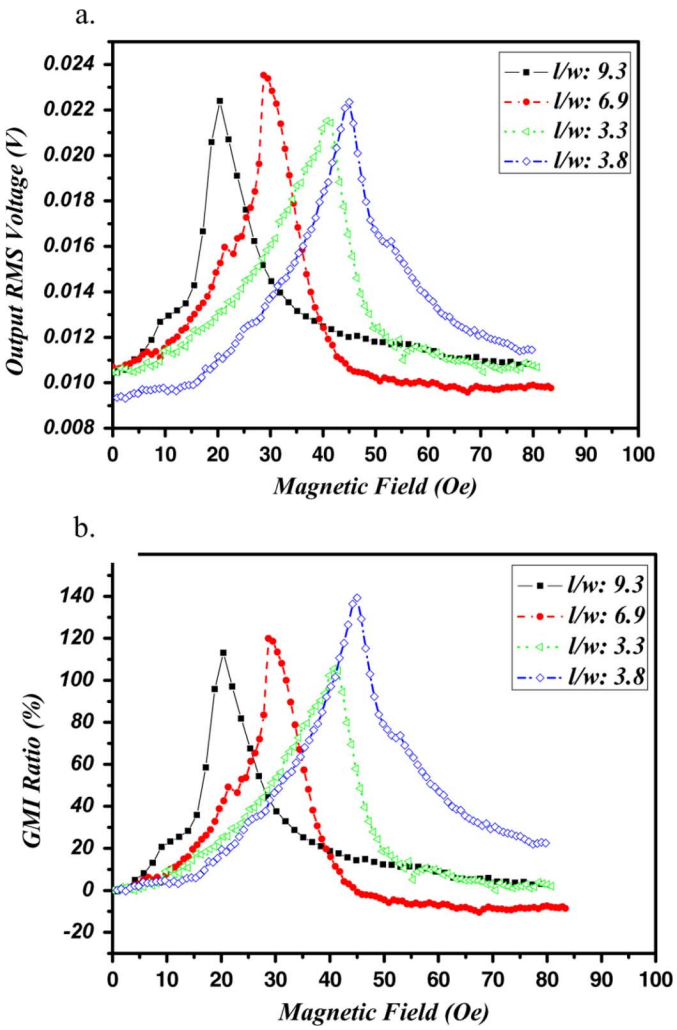

Fig. 2. Sensor characteristics of micron-scaled GMI devices. (a) Sensor output voltage with respect to the applied magnetic field. (b) GMI ratio in percentage.

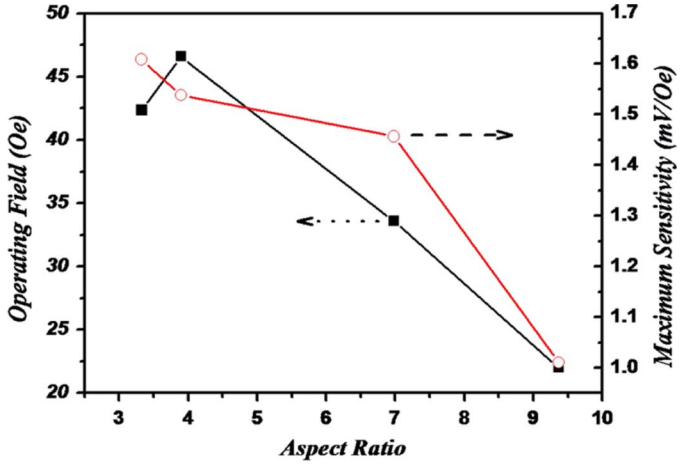

Fig. 3. Operating field and maximum sensitivity with respect to the aspect ratio of the GMI devices.

field was measured to be more than 110% as the ac source signal with a frequency of 20 MHz and 7-dBm power were applied.

It was found that the external field point where the rms voltage maximum occurs largely depends on the lateral aspect ratio of the devices. Since the rms voltage variation, hence, the impedance variation, is most rapid around this field point, the operating field of the devices is largely determined by this value. Beginning with 22 Oe of the operating field at the lateral aspect ratio of 9.3, it was increased up to 46.5 Oe at the aspect ratio of 3.8. The external field at impedance maximum is closely related to the device's anisotropy field. From classical electrodynamics based on Maxwell and Landau–Lifschitz–Gilbert equations, Usov N.A. *et al.* [12] showed that in the quasistatic limit, RF impedance maximum occurs approximately when the external field reaches the transverse anisotropic field of the material. As the transverse anisotropic field increases as the aspect ratio decreases due to reduced-shape anisotropy, this tendency is consistent with conventional millimeter-sized GMI sensors. However, compared to conventional GMI devices of which the typical aspect ratio is more than 20, the contribution of shape anisotropy to the maximum field point is substantially increased in micron-scaled GMI devices. From previous works, we have fabricated the $Co_{30}Fe_{34}Ni_{36}$ GMI device, which is 150 μm wide and 5 mm long (aspect ratio over 30) of which the maximum field point was measured to be about 18 Oe. Therefore, this result shows that a dramatic increase of the operating point for GMI devices in micron scale can be possible by reducing the lateral aspect ratio of the devices.

Moreover, the unique property of our micro sensors is that the maximum sensitivity, defined by output voltage variation per unit magnetic field, also increases as the aspect ratio decreases. Beginning with the lowest maximum sensitivity of 1 mV/Oe at the aspect ratio of 9.3, 1.6 mV/Oe was recorded approximately at the aspect ratio of 3.3. From the previous works [8], [9], [12], it was reported that the impedance maximum peak broadens as the operating field point increases; thus, maximum sensitivity decreases as the lateral aspect ratio decreases. Moreover, since previous theoretical works, such as [11], assume an infinite length along the wire axis, they exclude shape anisotropy and cannot explain the present result for micron-scaled devices. Therefore, further research is needed in order to successfully describe GMI characteristics when device length becomes comparable to the width so that shape anisotropy considerably affects total impedance variation. Nevertheless, this result shows that by adjusting the aspect ratio of GMI sensors, the achievement of high maximum sensitivity as well as the reasonable operation field is possible.

In order to clearly indicate sensor characteristics, the maximum sensitivity and operating field with respect to the aspect ratio are depicted in Fig. 3. The maximum operating field was achieved when the aspect ratio is 3.8 and maximum sensitivity was found to be 1.609 mV/Oe (15. 4%/Oe) at the aspect ratio of 3.3.

The measured maximum operating field and maximum sensitivity, to our best knowledge, are the highest value among the magnetic sensors for biological applications. In future works, the RF lock in the amplifier can be used to further reduce noise and increase resolution of the measurement system. Finally, from this investigation, one can conclude that in order to increase the operating field and maximum sensitivity, the

aspect ratio of 3.3–3.8 is the optimized value for micron-scaled $Co_{30}Fe_{34}Ni_{36}$ GMI sensors.

IV. Conclusion

In summary, we have demonstrated that the micron-scaled GMI sensors have advantages for an application to magnetic bead detection on the ground that one can increase the operating field and maximum sensitivity by adjusting the aspect ratio. Setting the optimized aspect ratio of 3.3–3.8, we have successfully fabricated ultra-high-sensitive micro GMI sensors with an overall GMI ratio of more than 110% and a maximum sensitivity of 1.609 mV/Oe (15.4%/Oe) at the operating field of 43.1 Oe. With these outstanding device characteristics, we will discuss the dynamic detection of a single micron-sized magnetic bead using the micro fluid channel in subsequent works.

Acknowledgment

This work was supported in part by a grant from the Fundamental R&D Program for Core Technology of Materials, funded by the Ministry of Commerce, and R&D Program for NT-IT Fusion Strategy of Advanced Technologies, Industry and Energy, Republic of Korea, and in part by KOSEF through the National Core Research Center for Nanomedical Technology.

References

[1] W. Shen, X. Liu, D. Mazumdar, and G. Xiao, "In situ detection of single micron-sized magnetic beads using magnetic tunnel junction sensors," *Appl, Phys. Lett.*, vol. 86, p. 253901, 2005.

[2] G. Li, V. Joshi, R. L. White, and S. X. Wang, "Detection of single micron-sized magnetic bead and magnetic nanoparticles," *J. Appl. Phys.*, vol. 93, p. 7557, 2003.

[3] O. Kazakova and J. Gallop, "Scanned micro-Hall microscope for detection of biofunctionalized magnetic beads," *Appl. Phys. Lett.*, vol. 90, p. 162502, 2007.

[4] "Ultralow impedance measurement using 2-port measurement," Agilent Technologies Appl. Note, 2007.

[5] L. V. Panina and K. Mohri, "Magneto-impedance effect in amorphous wires," *Appl. Phys. Lett.*, vol. 65, p. 1189, 2007.

[6] M. Knobel, M. L. Sánchez, C. Gómez-Polo, P. Marín, M. Vázquez, and A. Hernando, "Giant magneto-impedance effect in nanostructured magnetic wires," *J. Appl. Phys.*, vol. 79, p. 1646, 1996.

[7] H. Chiriac, M. Tibu, A.-E. Moga, and D. D. Herea, "Magnetic GMI sensor for detection of biomolecules," *J. Magn. Magn. Mater.*, vol. 293, p. 671, 2005.

[8] H. Chiriac, T. A. Óvári, and C. S. Marinescu, "Giant magneto-impedance effect in nanocrystalline glass-covered wires," *J. Appl. Phys.*, vol. 83, p. 6584, 1998.

[9] C. Garcia, J. Gonzalez, A. Chizhik, A. Zhukov, and J. M. Blanco, "Asymmetrical magneto-impedance effect in Fe-rich amorphous wires," *J. Appl. Phys.*, vol. 95, p. 6756, 2004.

[10] P. Ripka and L. Kraus, , P. Ripka, Ed., "Magnetoimpedance and magnetoinductance," in *Magnetic Sensors and Magnetometers*. Norwood, MA: Artech House, 2001, pp. 350–358.

[11] K. Mohri, T. Uchiyamaa, L. P. Shena, C. M. Caia, and L. V. Panina, "Amorphous wire and CMOS IC-based sensitive micro-magnetic sensors (MI sensor and SI sensor) for intelligent measurements and controls," *J. Magn. Magn. Mater.*, vol. 249, pp. 351–316, 2002.

[12] N. A. Usov, A. S. Antonov, and A. N. Lagar'kov, "Theory of giant magneto-impedance effect in amorphous wires with different types of magnetic anisotropy," *J. Magn. Magn. Mater.*, pp. 159–173, 1998.

[13] W. Y. Jeung, H. K. Kim, and J. O. Lee, "The effect of composition and current condition on magnetic properties of Co-Fe-Ni soft magnetic alloy," *J. Kor. Mag. Soc. Von.*, vol. 15, no. 4, pp. 241–245, 2005.

[14] W. Y. Jeung, H. K. Kim, and C. B. Park, "The effect of magnetic property according to size and orientation of crystal for electroplated Co-Fe-Ni alloys," *J. Kor. Mag. Soc.*, vol. 16, no. 5, pp. 249–254, 2006.

[15] H. K. Kim, D. W. Chun, J. H. Han, K. B. Kim, and W. Y. Jeung, "Effects of external magnetic field on magnetic properties and surface morphology of electrodeposited CoFe Ni alloys," *Phys. Stat. Sol. (a)*, vol. 204, no. 12, pp. 4104–4107, 2007.

[16] S. H. Park, D. W. Chun, J. H. Han, Y. H. Kim, and W. Y. Jeung, "Giant Magneto Impedance effects in Micro- Patterned CoFeBSi amorphous ribbons," *Phys. Stat. Sol. (a)*, vol. 204, no. 12, pp. 4071–4074, 2002.

[17] H. B. Lee, Y. S. Kim, and S. C. Yu, "Super-giant maneto impedance effect of a LC-rasonator using a glass-coated amorphous microwire," *J. Magn.*, vol. 7, pp. 160–164, 2002.

Manuscript received March 03, 2008. Current version published December 17, 2008. Corresponding author: W. Y. Jeung and W. Y. Lee (e-mail: wyjeung@kist.re.kr; wooyoung@yonsei.ac.kr).